Bulletin of the Mineral Research and Exploration

http://bulletin.mta.gov.tr

Determination of alteration zones applying fractal modeling and Spectral Feature Fitting (SFF) method in Saryazd porphyry copper system, central Iran

Behzad BEHBAHANI[a], Hamid HARATI[b*], Peyman AFZAL[c] and Mohammad LOTFI[a]

[a] *Islamic Azad University, Department of Geology, North Tehran Branch, Tehran, Iran*
[b] *Payame Noor University, Department of Geology, PO Box 19395-4697, Tehran, Iran*
[c] *Islamic Azad University, Department of Petroleum and Mining Engineering, South Tehran Branch, Tehran, Iran*

Research Article

Keywords:
Alteration, Spectral Feature Fitting (SFF) Method, Concentration-Area Fractal Model, Saryazd Porphyry System.

Received Date: 10.07.2021
Accepted Date: 13.03.2023

ABSTRACT

The target of this research is recognition of the alteration zones utilizing concentration-area fractal methodology according to the reflection of the main minerals of each alteration zone that enhanced by Spectral Feature Fitting (SFF) Method due to Advanced Space-borne Thermal Emission and Reflection Radiometer (ASTER) satellite images in Saryazd porphyry system, central Iran. The alterations and mineralization are developed in Eocene volcanics. Remote sensing results achieved by the SFF method and Concentration-Area (C-A) fractal modeling represent different parts of propylitic, argillic and phyllic alteration zones due to their intensity and pixel values. In addition, the results reveal that there is a ring-shaped structure in the alteration zones, which are correlated with results, derived from X-Ray Diffraction (XRD) analyses and field observations.

1. Introduction

Hydrothermal alteration and mineralized zones associated with porphyry mineralization systems were extended into wall rocks above and around intrusive bodies and their zoning could be an important exploration key to find mineralization in hydrothermal deposits (Pirajno, 2009). Remote sensing data have been utilized to recognize and mapping of different alteration zones. The potential of the recognition by remote sensing data was based on the wavelength variety and spectral power identification of their sensors (Abrams et al., 1983; Rutz-Armenta and Prol-Ledesma, 1998; Çorumluoğlu et al., 2015; Vural et al., 2015; Yazdi et al., 2018; Vural and Aydal, 2020). The short wave infrared (SWIR) spectral domain as an electromagnetic wavelength's portion is one of the essential implements for in recognizing different alteration zones (Sabins, 1999; Hewson et al., 2001; Tangestani and Moore, 2001; Sadeghi et al., 2013; Aramesh et al., 2015; Fakhari et al., 2019). In this study, the SFF method has been utilized to recognize these main minerals for alteration zones such as kaolinite, muscovite, chlorite and hematite. The different parts of the alteration zones were separated utilizing C-A fractal approach to find boundary of each alteration zone and classification them to boundary between each alteration zone and their classification to identify prospect area in Saryazd.

2. Regional Geology

The Urumieh-Dokhtar Magmatic Belt (UDMB) as an Andean-type magmatic arc extends for 2000 km

Citation Info: Behzad, B., Harati, H., Afzal, P., Lotfi, M. 2023. Determination of alteration zones applying fractal modeling and Spectral Feature Fitting (SFF) method in Saryazd porphyry copper system, central Iran. Bulletin of the Mineral Research and Exploration 172, 1-14. https://doi.org/10.19111/bulletinofmre.1264604

**Corresponding author: Hamid HARATI, hamid.harati437@yahoo.com*

from NW to SE and is considered as subduction-related calc-alkaline and alkaline rock masses (Berberian and King, 1981; Hassanzadeh, 1993; Ricou 1994; Moradian, 1997; Mohajjel et al., 2003; Alavi, 2004; Omrani et al., 2008; Agard et al., 2011). The major porphyry copper, molybdenum and gold ores in Iran occurred along the UDMB. Middle segment of the UDMB includes numerous porphyry-related copper deposits and prospects (Ahmadfaraj et al., 2019; Sabahi et al., 2019; Jebeli et al., 2020).

Three major periods of magmatism and associated Cu mineralization are identified along the UDMB during Eocene–Oligocene, Middle to Late Oligocene and Middle to Late Miocene episodes (Shahabpour and Kramers, 1987; Kirkham and Dunne, 2000; McInnes et al., 2005; Jahangiri 2007; Razique et al., 2007; Ahmadian et al., 2008; Ghorbani and Bezanjani, 2011; Asadi et al., 2014). Several Cu mineralization/ deposits in the UDMB were simultaneously formed during the emplacement of Miocene granodiorite to quartz-monzonite intrusions (Zarasvandi et al., 2015). Several porphyry deposits/occurrences were discovered in the central section of the UDMB such as Darreh Zereshk (Aghazadeh et al., 2015; Zarasvandi et al., 20015), Kahang (Afzal et al., 2012), Dali (Asadi Haroni and Sansoleimani, 2012; Ayati et al., 2013) and Zafarghand (Behbahani et al., 2013*a, b*).

2.1. Geology of Saryazd

The Saryazd porphyry system is situated in western border of the crustal central Iranian block, central Iran. There is an intersection between the UDMB and the Central Iranian block (Figure 1). The lithology of the Saryazd area consists Eocene volcanic rocks such as tuff breccia, tuff and devitrified pyroclastics, Olivine-pyroxene basalts, quartz porphyry to monzogranite and quartz monzodiorite porphyry intrusions with outcrops in SW part of the study area. These units infiltrated in volcanics and micritic limestones and thereby caused alteration and mineralization in volcanics. All these rocks are covered by Quaternary alluvial sediments. The main faults predominate in the center of the study area with a NNE - SSW trend in the studied area (Figure 2, Behbahani, 2017).

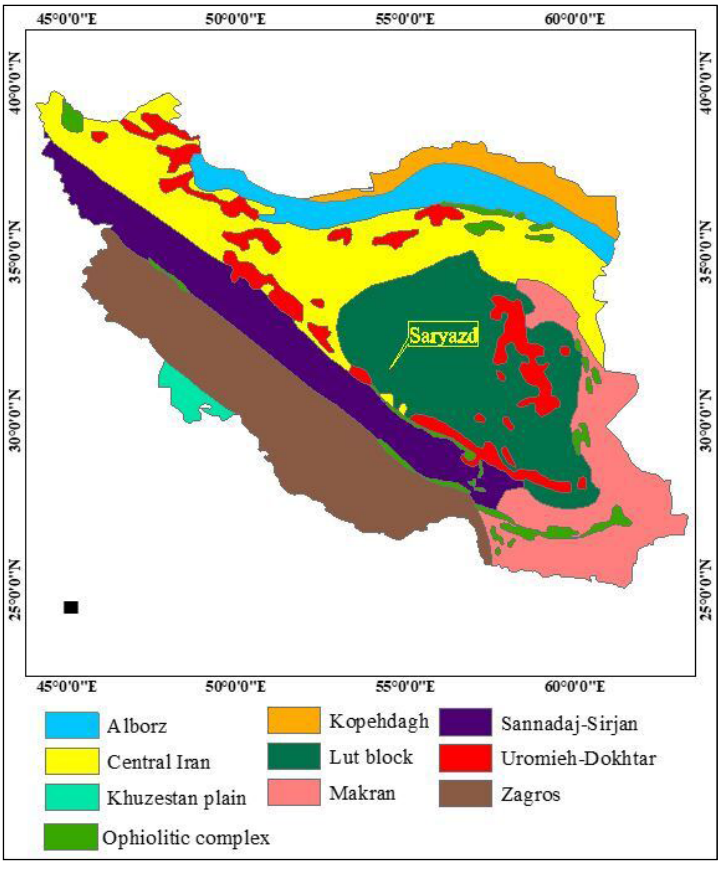

Figure 1- Main geological subdivisions of Iran (modified after Stöcklin, 1968, 1977; Nabavi, 1976).

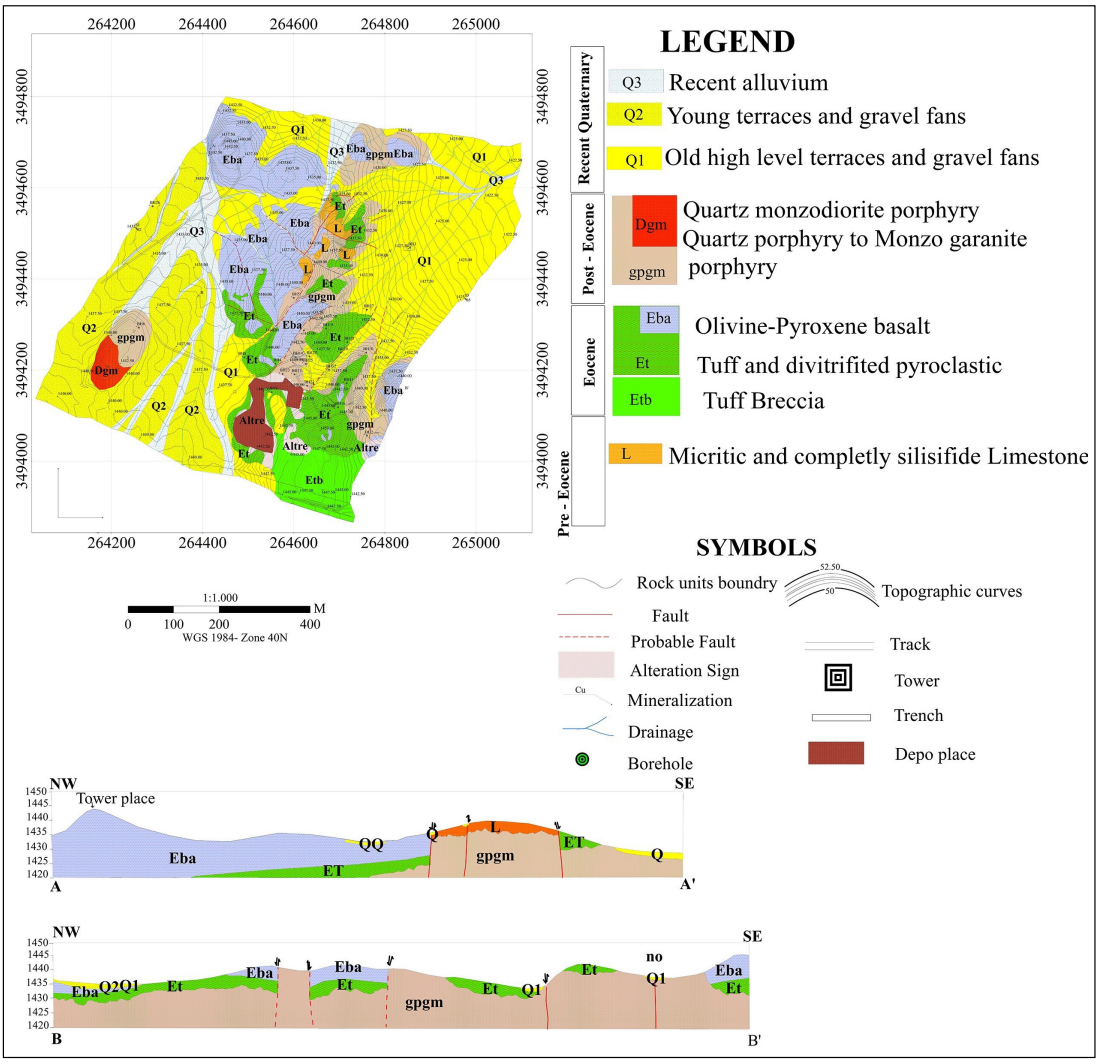

Figure 2- Geological map of the Saryazd system.

3. Methodology

3.1. Spectral Feature Fitting

The SFF method is an absorption feature based technique for corresponding image spectral to situation end members which improved by the U.S. Geological Survey (USGS; Clark et al., 1992; Kruse et al.,1993*a*, *b*; Kruse and Lefkoff, 1993, Swayze and Roger, 1995; Zamyad et al., 2019). Methodology for interpretation of hyper spectral data has still not directly recognized minerals. They represent similarity of a mineral to another known material. In addition, direct methods for identification of different minerals are based on specific spectral features extraction (Yamaguchi and Lyon, 1986; Clark et al., 1987; Kruse, 1988; 1990; Clark and Swayze, 1995). Moreover, the SFF method needs to reduce data to reflectance and remove a continuum from the reflectance data prior to analyses. A continuum is a mathematical function applied to isolate a particular absorption feature for analyses (Clark and Roush, 1984; Kruse et al., 1985; Clark et al., 1992).

3.2. Concentration-Area (C-A) Fractal Model

Cheng et al. (1994) established the C–A fractal model that is applied to detect background and anomalies for various data (pixel value in this scenario) as follows:

$$A(\rho \leq \upsilon) \propto \rho^{-\alpha_1} \boldsymbol{\rho}^{-\alpha_1};\ A(\rho \geq \upsilon) \propto \rho^{-\alpha_2} \boldsymbol{\rho}^{-\alpha_1}\, \boldsymbol{\rho}^{-\alpha_2}$$

The A (ρ) denotes the area with pixel values greater than the value ρ; υ indicates a threshold; and α_1 and α_2 are fractal dimensions. The breaking points between line segments on a C-A logarithmic plot and the corresponding values of ρ have been applied as thresholds to distinguish pixel values into various components, at the similar time showing different items, such as geological and geochemical differences (Goncalves et al., 2001; Lima et al., 2003; Aliyari et al., 2020). Cheng and Li (2002) utilized the C-A model for interpretation of Thematic mapper (TM) images in Mitchell - Sulphurets Cu - Au porphyry system, NW of Canada. Moreover, Afzal et al. (2012) used the fractal modeling for separation of different alteration zones in Khoshnameh area, central Iran. Zamyad et al. (2019) used fractal modeling for classification of alteration zones in Tirka copper mineralization (NE Iran).

4. Application of C-A Fractal Modeling

In this paper, the ASTER data in SWIR used to recognize the alteration zones in various Saryazd porphyry systems. First, the image was corrected and the ENVI 4.7 software and the SFF method was used to extract and map the spectrum of the kaolinite, muscovite, hematite and chlorite, which are the main alteration mineral of porphyry systems (Figure 3 and 4). The related pixels of alteration zones for main mineralization were enhanced and their values were

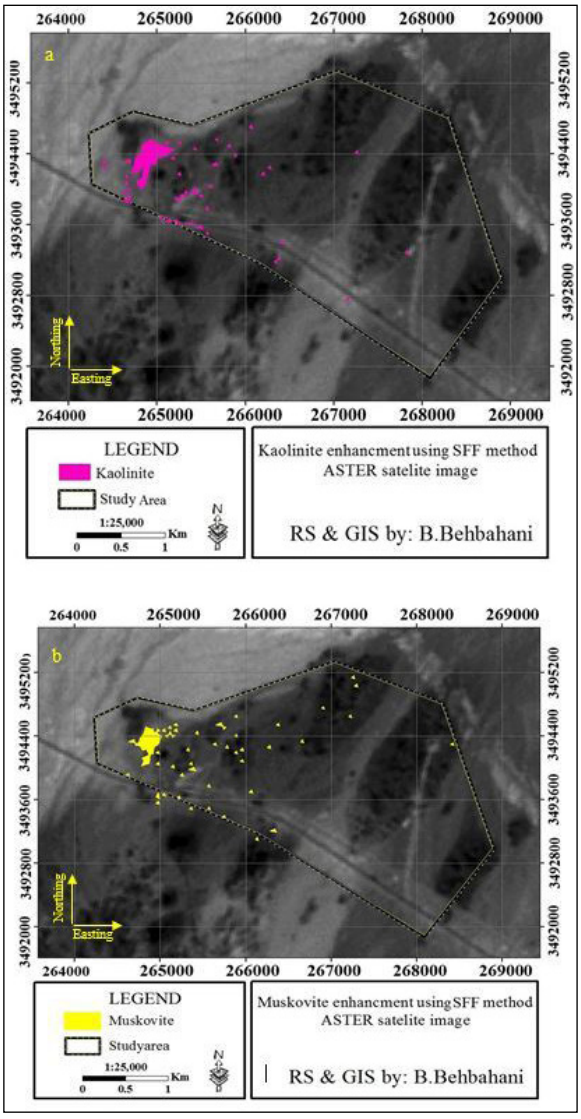

Figure 3- Main minerals of porphyry alteration enhanced by SFF method; a) kaolinite and b) muscovite.

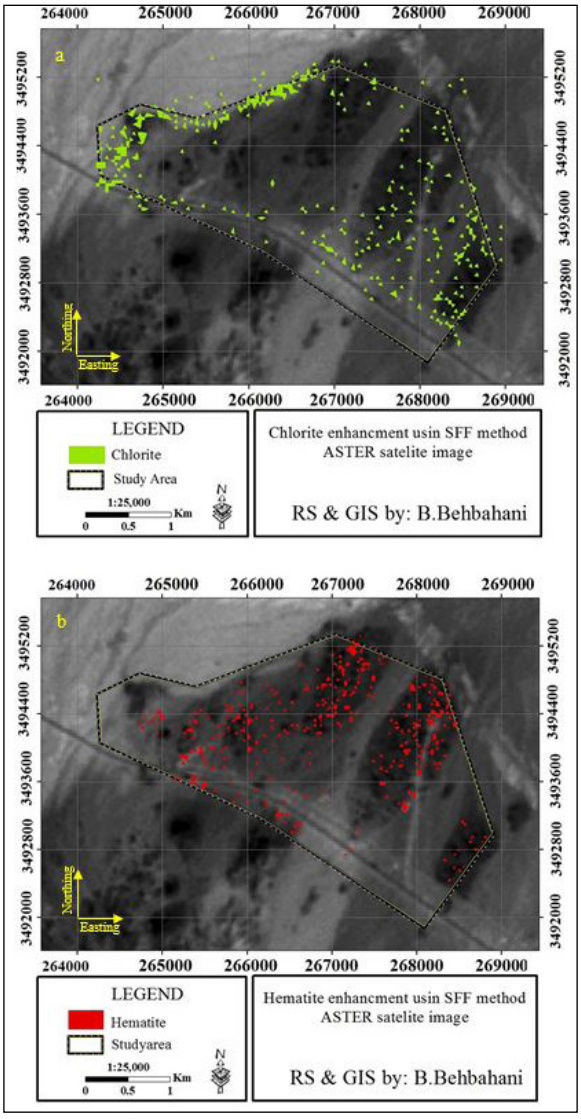

Figure 4- Main minerals of porphyry alteration enhanced by SFF method; a) hematite and b) chlorite.

reclassified using the C-A fractal model and log-log plots were produced for alteration zones (Figure 5 and 6). C-A log-log plot for kaolinite, the main mineral of the argillic alteration reveals five populations (Table 1). The first population is covering pixels by values lower than 31, which is distributed at the NW of the study area. Main populations occurring in the NW part of this area include values higher than 100. Moreover, the last population of kaolinite consists of the pixels by values, which are more than 158. This population includes pixels of the kaolinite at the NW and central sections of the Saryazd region (Figure 7a). Based on the fractal modelling, most parts of the argillic alteration zone are high intensity, which contain pixel values higher than 100. The C-A method for muscovite, being the main mineral of the phyllic alteration, reveals four fractal populations with the first population involving pixel values lower than 141. The main populations have pixel values higher than 186, which is situated at the NW portion of the study area. Furthermore, the last population for muscovite comprises pixel values more than 234 which is located at the NW of the Saryazd system (Figure 7b). The C-A method for chlorite reveals five populations that are distributed in the marginal parts of the studied area, as depicted in Figure 8a. Major populations of chlorite consist of pixel scores > 173 that are distributed in the NW, SE and central sections of the studied area. However, the final population of chlorite pixel values is situated at the NE and central parts of the study system and included the values more than 229. The C-A fractal modeling for hematite shows five major populations that contain pixel values higher than 173 in the SE and NW of the studied area. The last population of hematite pixel values are located in all the parts of the area, which are higher than 218 (Figure 8b).

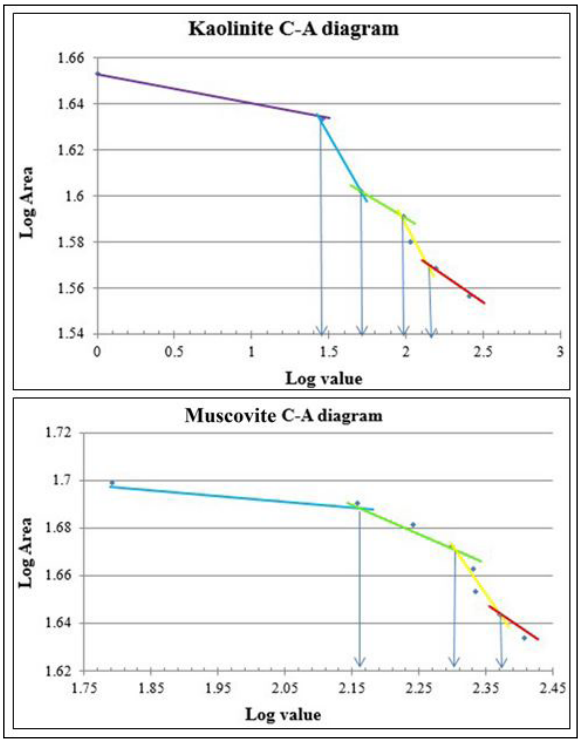

Figure 5- Log - Log plots for pixel values of kaolinite and muscovite.

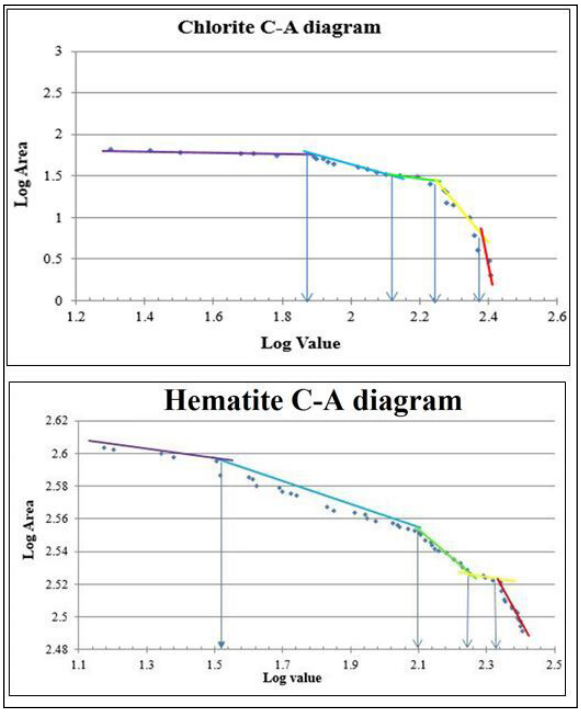

Figure 6- Log - Log plots for pixel values of chlorite and hematite.

Table 1- Specified population pixel values for alterations main minerals using C-A fractal model.

Mineral	1st population	2nd population	3rd population	4th population	5th population
Kaolinite	0-31	31-50	50-100	100-158	158<
Muscovite	0-141	141-186	186-234	234<	-
Chlorite	0-83	83-120	120-173	173-22	229<
Hematite	0-34	34-138	138-173	173-218	218<

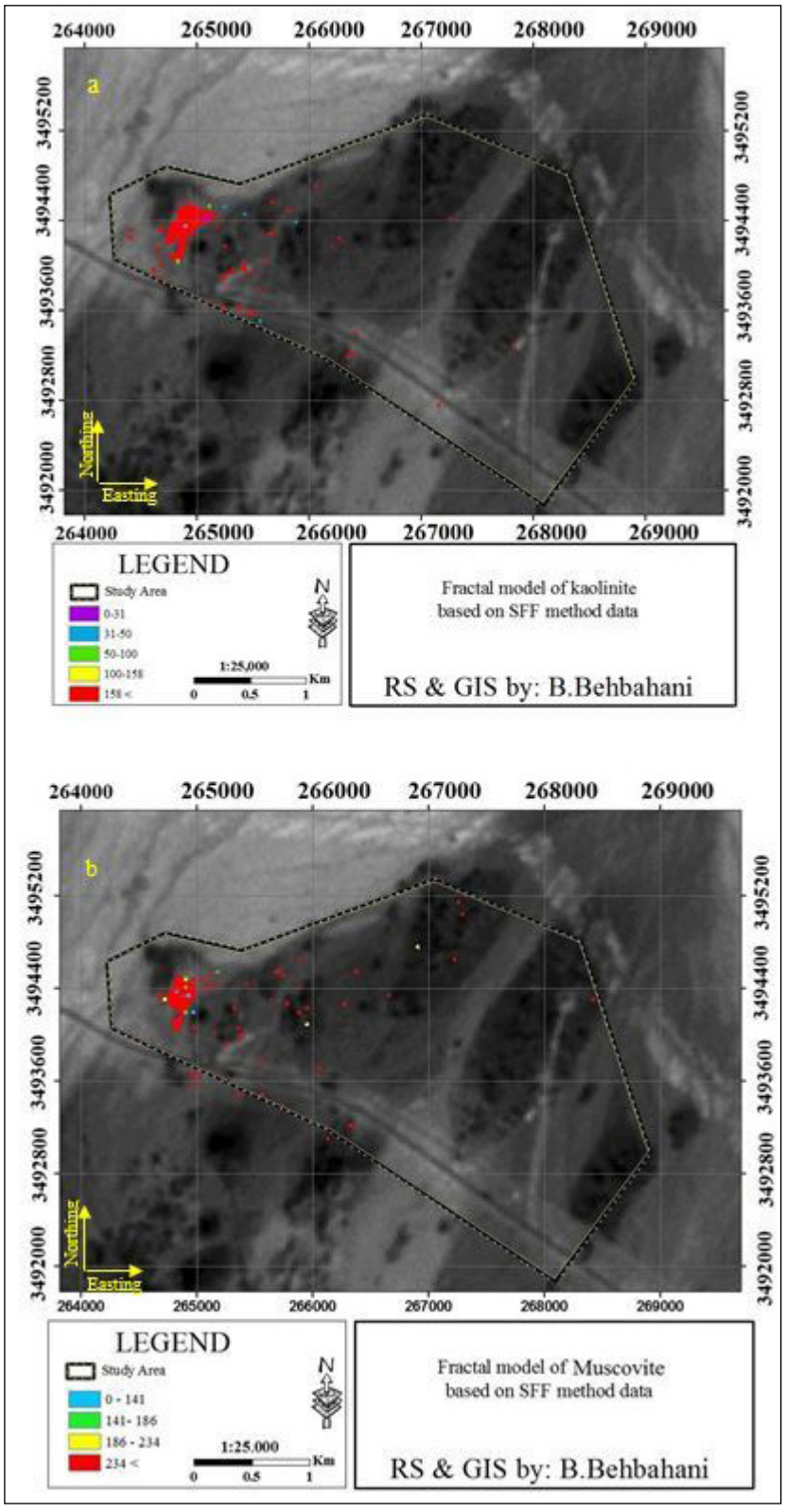

Figure 7- C-A fractal model for; a) kaolinite and b) muscovite pixel values based on SFF method data in 314 the Saryazd porphyry system.

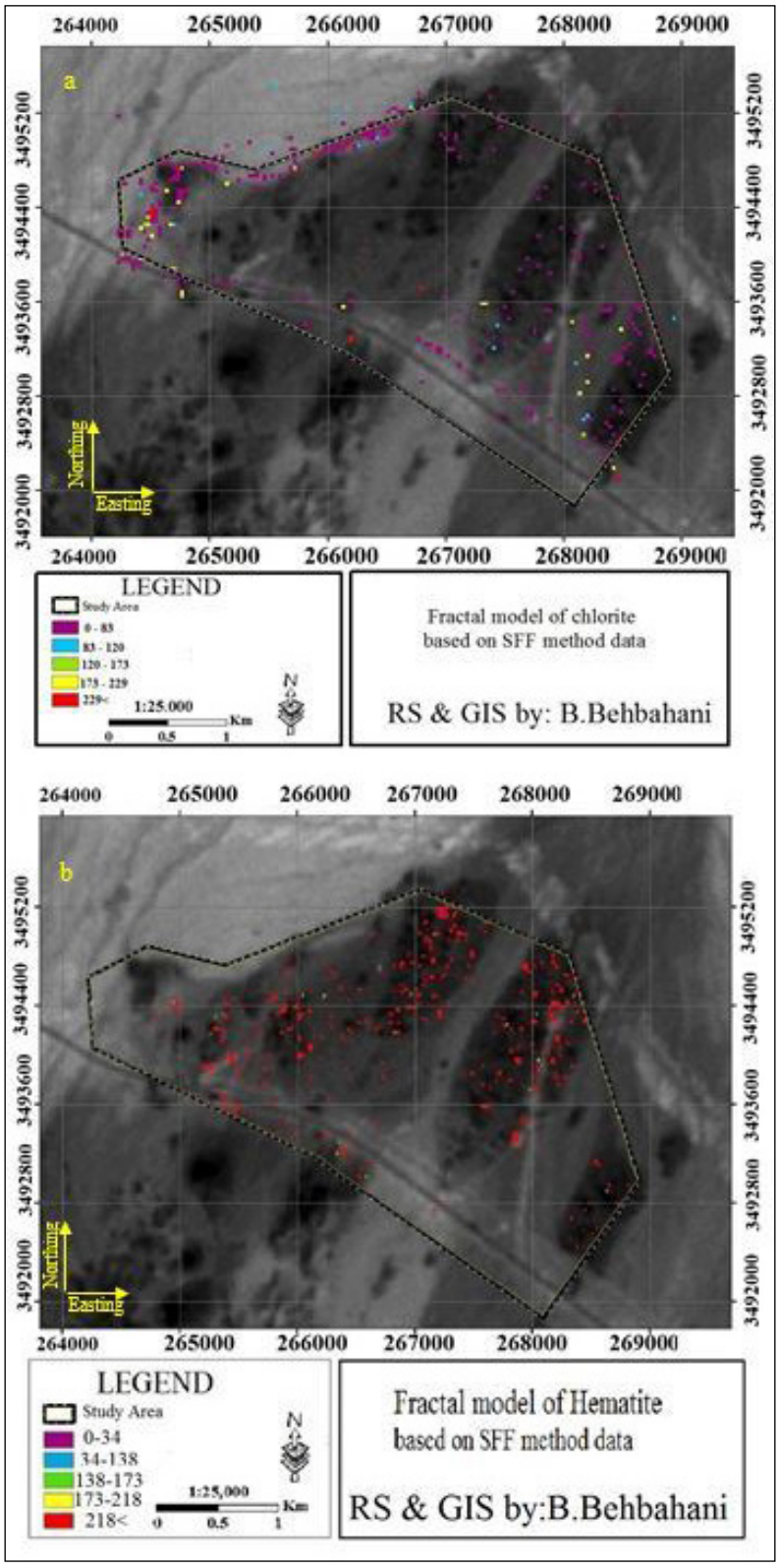

Figure 8- C-A fractal model for; a) chlorite and b) hematite pixel values based on SFF method data in the 345 Saryazd porphyry system.

5. Validation Result with Geological Characteristics

XRD is an appropriate method for mineral analyses (Faheem et al., 2015; Gold et al., 1983). In this research, 21 samples of XRD data were used to determine the minerals of the alteration zones, (Table 1 and Figure 9), thereby determining the accuracy of remote sensing results and the C-A in the Saryazd area (Figure 10). The comparison between the XRD results and C-A fractal modeling shows that pixels marked as high intensity alteration zones are correlated with the altered samples, as depicted in Table 1. Some samples like STZ12 have a series of the main alteration minerals consisting of argillic, phyllic and iron oxide (Table 2).

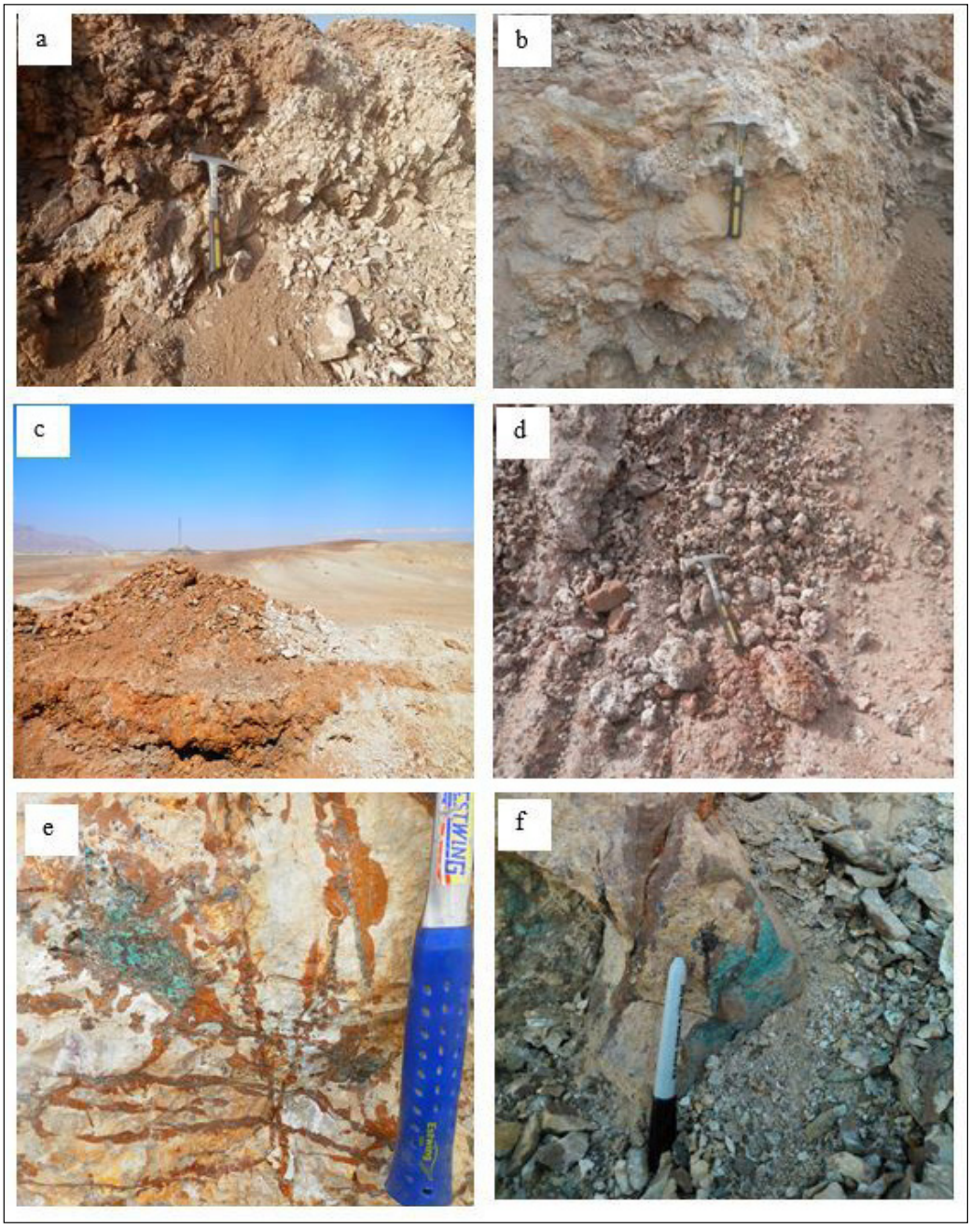

Figure 9- Altered and mineralized parts of the studied area; a) argillic alteration, b) advanced argillic and 348 phylic alterations, c) iron oxide mineralization as siderite, goethite and limonite, d) hematite and argillic 349 alteration, e) stock work structure and mineralization as goethite and malachite which is accorded in 350 Crossed streaks, f) Cu and Fe oxide mineralization in border of Saryazd porphyry system.

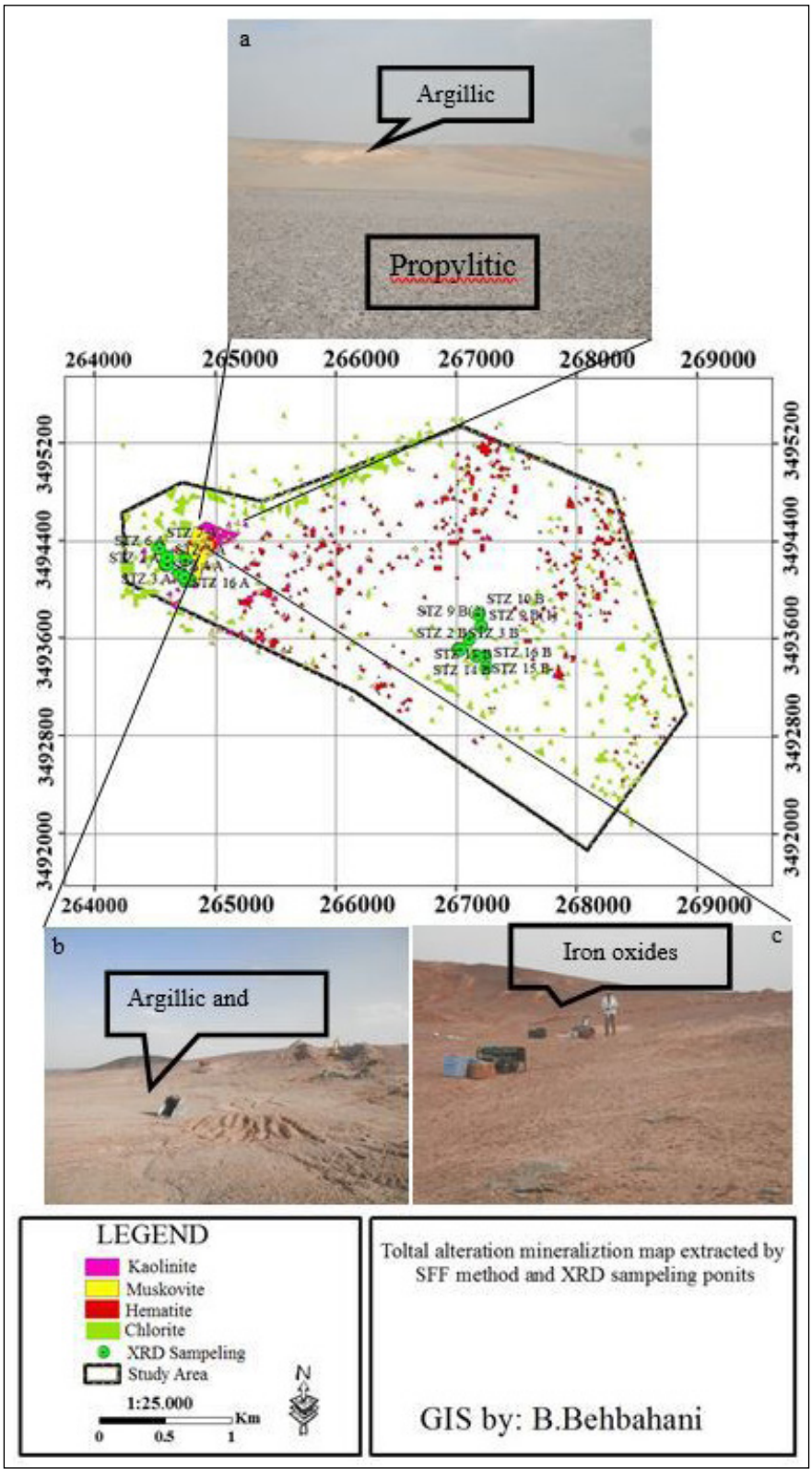

Figure 10- The correlation map of the XRD sampling by ground geology and remote sensing The images 385 show the alteration zones in the data in the Saryazd district; a) argillic and propylitic, b) argillic and 386 phylic, c) Iron oxide alterations out crops.

Table 2- XRD analysis results for alterations of the Saryazd porphyry system.

Samples	Major Phase(s)	Minor Phase(s)
STZ 1 A	Quartz Albite Orthoclase ($KAlSi_3O_8$)	Muscovite-Illite
STZ 2 A	Quartz Albite Orthoclase	Muscovite-Illite Montmorillonite
STZ 3 A	Quartz Albite Orthoclase	Illite
STZ 4 A	Quartz Orthoclase Barite	Kaolinite
STZ 5 A	Quartz Orthoclase	Kaolinite Barite
STZ 6 A	Quartz Albite Orthoclase	Muscovite-Illite
STZ 7 A	Quartz Albite Orthoclase	Muscovite-Illite Calcite Kaolinite Montmorillonite
STZ 10 A	Quartz Orthoclase Montmorillonite Albite	Kaolinite Muscovite-Illite
STZ 12 A	Quartz	Orthoclase Muscovite-Illite Kaolinite Hematite
STZ 14 A	Orthoclase Quartz	Kaolinite Hematite
STZ 15 A	Quartz Orthoclase	Albite Muscovite-Illite Chlorite
STZ 16 A	Albite Quartz Orthoclase	Calcite Kaolinite Muscovite - Illite
STZ 2 B	Quartz Albite Calcite Orthoclase	Kaolinite Muscovite-Illite Dolomite
STZ 3 B	Albite Quartz Calcite	Chlorite Muscovite-Illite
STZ 9 B(1)	Albite Quartz Calcite	Chlorite Muscovite-Illite
STZ 9 B(2)	Quartz Albite Calcite Microcline	Muscovite-Illite
STZ 10 B	Quartz Gypsum Anhydrite	Bassanite Kaolinite Muscovite-Illite
STZ 11 B	Albite Orthoclase Quartz	Kaolinite Hematite
STZ 14 B	Quartz Albite Orthoclase	Calcite Muscovite-Illite Kaolinite Hematite
STZ 15 B	Quartz Orthoclase	Muscovite- Illite Kaolinite
STZ 16 B	Halite	Gypsum Quartz Anhydrite Muscovite-Illite

6. Conclusions

According to the results derived from the C-A fractal modeling and SFF method on the remote sensing data, the high intensity alteration zones were located in the NW of the Saryazd area. The argillic and phyllic alteration zones (kaolinite-muscovite) predominate in this part of the study area where the major Cu mineralization occurs. As mentioned before, the high pixels, which are enhanced by the SFF method, are related to the chlorite. The pixel value of the chlorite is higher than the others, which is the margin of the porphyry system. Moreover, the XRD analyses of the alteration samples validated the results obtained from the SFF and fractal analysis. Consequently, the C-A approach for pixels extracted by the SFF method identified a ring structure in alteration zones, which may also indicate a porphyry mineralization.

References

Abrams, M. J., Brown, D., Lepley, L., Sadowski, R. 1983. Remote sensing for porphyry copper deposits in southern Arizona. Economic Geology 78(4), 591-604.

Afzal, P., Fadakar Alghalandis, Y., Moarefvand, P., Rashidnejad Omran, N., Asadi, H. 2012. Application of power -spectrum – volume fractal method for detecting hypogene, supergene enrichment, leached and barren zones in Kahang porphyry Cu deposit, Central Iran. Journal of Geochemical Exploration 112, 131-138.

Agard, P., Omrani, J., Jolivet, L., Whitechurch, H., Vrielynck, B., Spak-man, W., Monié, P., Meyer, B., Wortel, R., 2011. Zagros orogeny: a subduction-dominated process. Geological Magazine 148, 692–725.

Aghazadeh, M., Houb, Z.G., Badrzadeh, Z., Zhou, L. 2015. Temporal – spatial distribution and tectonic setting of porphyry copper deposits in Iran: constraints from zircon U–Pb and molybdenite Re–Os geochronology. Ore Geology Reviews.

Ahmadian, J., Haschke, M., McDonald, I., Regelous, M., Ghorbani, M. R., Emami, M., Murata, M., 2008. High magmatic flux during Alpine–Himalayan collision: constraints from the Kal-e-Kafi complex, central Iran. Geological Society of America Bulletin.

Ahmadfaraj, M., Mirmohammadi, M., Afzal, P., Yasrebi, A. B., Carranza, E. J., 2019. Fractal modeling and fry analysis of the relationship between structures and Cu mineralization in Saveh region, Central Iran. Ore Geology Reviews 107, 172-185.

Alavi M. 2004. Regional stratigraphy of the Zagros fold - thrust belt of Iran and its proforeland evolution. American Journal of Science 304, 1–20.

Aliyari, F., Afzal, P., Lotfi, M., Shokri, S., Feizi, H. 2020. Delineation of geochemical haloes using the developed zonality index model by multivariate and fractal analysis in the Cu – Mo porphyry deposits. Applied Geochemistry 121, 104694.

Aramesh Asl, R., Afzal, P., Adib, A., Yasrebi, A. 2015. Application of multifractal modeling for the identification of alteration zones and major faults based on ETM+ multispectral data. Journal of the Indian Society of Remote Sensing 43(1), 121-132.

Asadi, S., Moore, F., Zarasvandi, A. 2014. Discriminating productive and barren porphyry copper deposits in the southeastern part of the central Iranian volcano-plutonic belt, Kerman region, Iran: a review. Earth Science Reviews 138, 25-46.

Asadi Haroni, H., Sansoleimani, A. 2012. Prospecting activities at Dalli Cu - Au porphyry deposit, central province of Iran, Iran. Lahijan Research Journal, University of Lahijan 15(6), 34-46 (in Persian with English abstract).

Ayati, F., Yavuz, F., Asadi, H. H., Richards, J. P., & Jourdan, F. 2013. Petrology and geochemistry of calc-alkaline volcanic and subvolcanic rocks, Dalli porphyry copper–gold deposit, Markazi Province, Iran. International Geology Review, 55(2), 158-184.

Behbahani, B. 2017. Presentation a genetic and exploratory model in Saryazd copper deposit (central Iran) based on geology, geochemical, geophysical and fluid inclusion data. PhD Thesis, Islamic Azad University North Tehran branch, 185.

Behbahani, B., Afzal, P., Jafari, M. R., Asadi harooni, H., Ajayebi, K. S., Noori, R. 2013*a*. Remote sensing studies in Zafarghand porphyry system for reconnaissance of prospects. Lahijan Research Journal, University of Lahijan 2(6), 1-10 (in Persian).

Behbahani B., Afzal P., Jafari M. R., Asadi harooni H., Ajayebi K. S. 2013*b*. Geophysical and Geochemical anomaly separation by concentration-area fractal model in Zafarghand Cu-Mo porphyry deposit, Isfahan province. Journal of the Earth, Islamic Azad University North Tehran 8(30), 25-37 (in Persian with English abstract).

Berberian, M., King, G. C. 1981. Towards a paleogeography and tectonic evolution of Iran.Canadian Journal of Earth Sciences 18, 210–265.

Cheng, Q., Agterberg, F. P., Ballantyne, S. B. 1994. The separation of geochemical anomalies from background by fractal methods, Journal of Geochemical Exploration, 51, 109-130

Cheng, Q., Li, Q. 2002. Fractal concentration - area method for assigning a color palette for image representation. Computers and Geosciences 28, 567-575.

Clark, R. N., and Roush,T. L. 1984. Reflectance spectroscopy: quantitative analyses techniques for remote sensing applications, Journal of Geophysical Research 89(7), 6329-6340.

Clark, R. N., King, T.V., Gorelick, N. S. 1987. Automatic continuum analyses of reflectance spectra: in Proceedings, Third AIS workshop, 2- 4 June 1987, JPL Publication, Jet Propulsion Laboratory, Pasadena, California, 138-142.

Clark, R. N., Swayze, G. A., Gallagher, A. 1992. Mapping the mineralogy and lithology of Canyonlands, Utah with imaging spectrometer data and the multiple spectral feature-mapping algorithm. In: Summaries of the Third Annual JPL Airborne Geoscience Workshop, JPL Publication 92-14, 1, 11–13.

Clark, R. N., Swayze, G. A. 1995. Mapping minerals, amorphous materials, environmental materials, vegetation, water, ice, and snow, and other materials: the USGS tricorder Algorithm. In: Summaries of the Fifth Annual JPL Airborne Earth Science Workshop, JPL Publication 95(1), 39–40.

Çorumluoğlu, O., Vural, A., Asri, I. 2015 Determination of Kula basalts (geosite) in Turkey using remote sensing techniques Journal of Arabian Geosciences 8, 10105–10117.

Faheem, M., Giridharan, R., Liang, Y., Van Der, P. 2015. Micro - XRD characterization of a Single Copper filled through Silicon. Journal of Materials Letters.

Fakhari, S., Jafarirad, A., Afzal, P., Lotfi, M. 2019. Delineation of hydrothermal alteration zones for porphyry systems utilizing ASTER data in Jebal - Barez area, SE Iran. Iranian Journal of Earth Sciences 11 (1), 80-92.

Ghorbani, M. R., Bezanjani, R. N. 2011. Slab partial melts from the metasomatizing agent to adakite, Tafresh Eocene volcanic rocks, Iran. Island Arc 20, 188–202.

Gold C. M., Cavell P. A., Smith D. G. W. 1983. Clay minerals in mixtures: samples preparation, analyses, and statistical interpretation. Clays and Clay Minerals 31(3), 191-199.

Goncalves, M. A., Mateus, A., Oliveira, V. 2001. Geochemical anomaly separation by multifractal modeling. Journal of Geochemical Exploration 72, 91–114.

Hassanzadeh J. 1993. Metallogenic and tectonomagmatic events in the SE sector of the Cenozoic active continental margin of central Iran (Shahr e Babak area, Kerman Province). PhD Thesis, University of California, Los Angeles (unpublished).

Hewson, R. D., Cudahy, T. J., Hunting, J. F. 2001. Geologic and alteration mapping at Mt Fitton, South Australia, using ASTER satellite - borne data. Institute of Electrical and Electronics Engineers 2, 724-726.

Jahangiri, A. 2007. Post-collisional Miocene adakitic volcanism in NW Iran: Geochemical and geodynamic implications. Journal of Asian Earth Sciences (30), 433–447.

Jebeli, M., Afzal, P., Pourkermani, M., Jafarirad, A. 2020. Characteristics of fluid inclusions in the Cenozoic volcanic - hosted Kushk-e-Bahram Manto - type Cu deposit of central Iran. Geologos 26 (2), 127-137.

Kirkham, R. V., Dunne, K. P. 2000. World distribution of porphyry, porphyry-associated skarn, and bulk - tonnage epithermal deposits and occurrences. Geological Survey of Canada 3792, 26.

Kruse, F. A. 1988. Use of Airborne Imaging Spectrometer data to map minerals associated with hydrothermally altered rocks in the northern Grapevine Mountains, Nevada and California. Remote Sensing of Environment 24(1), 31-51.

Kruse, F. A. 1990. Artificial intelligence for nalyses of imaging spectrometer Data: Proceedings, ISPRS Commission VII, Working Group 2 analyses of high spectral resolution imaging data. 17 - 21 September 1990, Canada, 59 -68.

Kruse, F. A., Lefkoff, A. B. 1993. Knowledge - based geologic mapping with imaging spectrometers. Remote Sensing Reviews, Special Issue on NASA Innovative Research Program (IRP) results, 8, 3-28.

Kruse, F. A., Raines, G. L., Watson, K. 1985. Analytical techniques for extracting geologic information from multichannel airborne spectroradiometer and airborne imaging spectrometer data: in Proceedings, International Symposium on Remote

Sensing of Environment, Thematic Conference on Remote Sensing for Exploration Geology, 4th Thematic Conference, Environmental Research Institute of Michigan, Ann Arbor, 309-324.

Kruse, F. A., Lefkoff, A. B., Boardman, J. W., Heidebrecht, K. B., Shapiro, A. T., Barloon, J. P., Goetz, A. F. H. 1993*a*. The spectral image processing system (SIPS) - interactive visualization and analyses of imaging spectrometer data. Remote Sensing of Environment 44, 145-163.

Kruse, F. A., Lefkoff, A. B., Dietz, J. B. 1993*b*. Expert System-Based Mineral Mapping in northern Death Valley, California/Nevada using the Airborne Visible/Infrared Imaging Spectrometer (AVIRIS). Remote Sensing of Environment, Special issue on AVIRIS 44, 309-336.

Lima, A., De Vivo, B., Cicchella, D., Cortini, M., Albanese, S. 2003. Multifractal inverse distance weighting interpolation and fractal filtering method in environmental studies: an application on regional stream sediments of (Italy), Campania region. Applied Geochemistry 18, 1853-1865.

McInnes, B. I. A., Evans, N. J., Fu, F. Q., Garwin, S. 2005. Application of thermochronology to hydrothermal ore deposits. Reviews in Mineral Geochemistry 58, 467-498.

Mohajjel, M., Fergusson, C.L., Sahandi, M.R. 2003. Cretaceous – Tertiary convergence and continental collision, Sanandaj - Sirjan Zone, Western Iran. Journal of Asian Earth Sciences 21, 397–412.

Moradian, A. 1997. Geochemistry, geochronology and petrography of feldspathoid bearing rocks in Urumieh-Dokhtar Volcanic Belt, Iran. PhD Thesis, University of Wollongong, 412, Australia.

Nabavi, M. H. 1976. An introduction to geology of Iran (in Persian). Geological Survey of Iran, Tehran.

Omrani, J., Agard, P., Whitechurch, H., Benoit, M., Prouteau, G., Jolivet, L. 2008. Arcmagmatism and subduction history beneath the Zagros Mountains, Iran: a new report of adakites and geodynamic consequences. Lithos 106, 380–398.

Pirajno, F. 2009. Hydrothermal Processes and Mineral Systems. Geological Survey of Western Australia, Springer, 111-114

Razique, A., Lo Grasso, G., Livesey, T. 2007. Porphyry copper – gold deposits at Reko Diq complex, Chagai Hills Pakistan. Proceedings of Ninth Biennial Society for Geology Applied to Mineral Deposits Meeting, Dublin.

Ricou, L. E. 1994. Tethys reconstruction: plates, continental fragments and their boundaries since 260 Ma from Central America to SoutheASTERn Asia. Geodinamica Acta (Paris) 7, 169–218.

Rutz-Armenta, J. R., Prol-Ledesma, R. M. 1998. Techniques for enhancing the spectral response of hydrothermal alteration minerals in thematic mapper images of central Mexico. International Journal of Remote Sensing 19, 1981–2000.

Sabahi, F., Afzal, P., Lotfi, M., Nezafati, N. 2019. Geological, fluid inclusion and isotopic characteristics of the Gardaneshir Zn – Pb deposit, central Iran. Geopersia 9 (2), 221-232.

Sabins, F. F. 1999. Remote sensing for mineral exploration. Ore geology reviews, 14(3-4), 157-183.

Sadeghi, B., Khalajmasoumi, M., Afzal, P., Moarefvand, P., Yasrebi, A. B., Wetherelt, A., Foster, P., Ziazarifi, A. 2013. Using ETM+ and ASTER sensors to identify iron occurrences in the Esfordi 1:100.000 mapping sheet of central Iran. Journal of African Earth Sciences 103–114.

Shahabpour, J., Kramers, J. D. 1987. Lead isotope data from the Sar Cheshmeh porphyry copper deposit, Kerman, Iranian Mineral Deposit 22, 278-281.

Stöcklin, J. 1968. Structural history and tectonics of Iran: a review. American Association of Petroleum Geologists Bulletin 52(7), 1229-1258.

Stöcklin, J. 1977. Structural correlation of the Alpine ranges between Iran and central Asia.

Swayze, G. A., and Roger N. C. 1995. Spectral identification of minerals using imaging spectrometry data: evaluating the effects of signal to noise and spectral resolution using the Tricorder Algorithm." Summaries of the 5th Annual JPL Airborne Earth Science Workshop.

Tangestani, M. H., Moore, F. 2001. Comparison of three principal component analyses techniques to porphyry copper alteration mapping: a case study in Meiduk area, Kerman, Iran. Canadian Journal of Remote Sensing 27,176–182.

Vural, A., Corumluoglu, O., Asri, I. 2015. Exploring Gördes zeolite sites by feature oriented principle component analysis of LANDSAT images. Caspian Journal of Environmental Sciences, 14(14), 285-298.

Vural, A., Aydal, D. 2020. Determination of Lithological Differences and Hydrothermal Alteration Areas by Remote Sensing Studies: Kısacık (Ayvacık-Çanakkale, Biga Peninsula, Turkey). Journal of Engineering Research and Applied Science

Journal of Engineering Research and Applied Science

Yamaguchi, Y., Lyon, R. J. P. 1986. Identification of clay minerals by feature coding of near - infrared spectra, Reno, Nevada, America.

Yazdi, Z., Jafarirad, A., Aghazadeh, M., Afzal, P., 2018. Alteration mapping for Porphyry copper exploration using ASTER and QuickBird multispectral images, Sonajeel Prospect, NW Iran. Journal of the Indian Society of Remote Sensing 46(10), 1581-1593.

Zamyad, M., Afzal, P., Pourkermani, M., Nouri, R., Jafari, M. R. 2019. Determination of hydrothermal alteration zones using remote sensing methods in Tirka area, Toroud, NE Iran. Journal of the Indian Society of Remote Sensing 47(11), 1817-1830.

Zarasvandi, A., Rezaci, M., Sadeghi, M., Lentz, D., Adelpour, M., Pourkaseb, H. 2015. Rare earth element signatures of economic and sub-economic porphyry copper systems in Urumieh-Dokhtar Magmatic Arc (UDMA), Iran. Ore Geology Reviews, 1428.